Estuarine, Coastal and Shelf Science 233 (2020) 106507

Contents lists available at ScienceDirect

Estuarine, Coastal and Shelf Science

journal homepage: http://www.elsevier.com/locate/ecss

Acceleration loggers reveal fine-scale heterogeneity in wave exposure along an open coast

Rebeca C. Focht [a,b,*], Jeffrey S. Shima [a,b]

[a] School of Biological Sciences, PO Box 600, Victoria University of Wellington, Wellington, New Zealand
[b] Victoria University Coastal Ecology Lab, 396 The Esplanade, Island Bay, Wellington, New Zealand

ARTICLE INFO

Keywords:
Wave exposure
Time series
Cost-effective method
Intertidal
Shallow subtidal
Fine scale

ABSTRACT

Wave action shapes species distributions and ecological interactions within the intertidal- and shallow-subtidal zone. Empirical estimates of wave exposure within these zones are limited by logistical constraints and/or cost. Hydrodynamic models of wave action poorly resolve fine-scale heterogeneity in wave energetics that are important for biology. We used cost-effective accelerometers to continuously measure fine-scale wave exposure across 12 locations (i.e., two depth strata at each of six sites), over sixteen consecutive months. We categorised wave exposure at each of our sites *a priori* (as 'exposed' or 'sheltered') based on shore topography. We compared *in situ* measurements of acceleration with a nearby wave rider buoy and evaluated variation in water acceleration and frequency of large wave events among sites and between depths. Wave height data significantly correlated with accelerometer data confirming accelerometers sufficiently measure wave action. Our analyses indicate significant fine-scale variation in acceleration, and differences in timing and frequency of large wave events during the study period. *In situ* acceleration had limited correspondence with shore-based (*a priori*) assessments of wave exposure. These results demonstrate the spatial and temporal differences in water acceleration on the Wellington south coast and highlight the limitations of surface topography to predict fine-scale wave action. This study also emphasizes the need for fine scale wave action measurements to better explain patterns in intertidal/shallow subtidal organism traits.

1. Introduction

Wave action can shape phenotypes (Denny, 2006), early life histories (Speransky et al., 2000; Crimaldi et al., 2002; Taylor et al., 2010), and ecological interactions (Connell, 1978; Menge and Sutherland, 1987; Harley and Helmuth, 2003) of species that inhabit shallow sub-tidal and/or intertidal zones. Empirical observations of wave action in these near-shore zones can be difficult and costly to obtain, and many studies use proxies (e.g., shoreline topography, wind, fetch, or wave height data from offshore buoys; Burrows, 2012; Jones et al., 2015; Caiger, 2017) to infer local wave exposures. These proxies poorly characterize the wave action experienced by organisms in particular locations along a coastline (Helmuth et al., 2010) because nearshore coastal features can create biologically important heterogeneity in wave action (e.g., Denny et al., 2003; Stevens et al., 2008). Hydrographic models used to predict localized wave action may be limited in their ability to incorporate underwater topographic features (e.g., boulders, pinnacles, etc.; Jones, 2014). Consequently, such models may fail to predict fine-scale heterogeneity in wave action (O'Donnell and Denny, 2008).

Dynamometers (Bell and Denny, 1994) and clod cards (Doty, 1971) can provide localised estimates of wave action in the intertidal zone and can characterize heterogeneity at finer spatial scales (Jokiel and Morrissey, 1993; Bell and Denny, 1994; Gaylord, 2000; Stevens et al., 2008; Tam, 2012). However, these methods can only provide relative (and time-integrated) estimates of wave exposure; they are not able to capture a high-resolution time-series of water acceleration. Wave rider buoys (Holthuijsen and Herbers, 1986) and Acoustic Doppler Current Profilers (ADCPs) can provide detailed information about currents and water velocity over time (Chang et al., 2011), but they are expensive to maintain and are not easily deployed in the intertidal zone. Previous studies have used Onset Hobo Pendant G acceleration loggers (UA-004-64) to measure wave action, as they are comparatively inexpensive, can be deployed in the intertidal zone, and record multiple measurements over time (Evans and Abdo, 2010; Figurski et al., 2011; Greene et al., 2012; Marchant et al., 2014; de Bettignies et al., 2015;

* Corresponding author. School of Biological Sciences, PO Box 600, Victoria University of Wellington, Wellington, New Zealand.
E-mail address: rebecafocht@gmail.com (R.C. Focht).

https://doi.org/10.1016/j.ecss.2019.106507
Received 9 April 2019; Received in revised form 13 October 2019; Accepted 27 November 2019
Available online 29 November 2019

Radermacher et al., 2015).

The Wellington south coast (North Island, New Zealand) is exposed to the Cook Strait, which frequently experiences strong winds and large swells generated by storms in the Southern Ocean (Bowman et al., 1983; Harris, 1990; Lewis et al., 1994). Storms can travel quickly up the South Island of New Zealand to cause a 3-m increase in significant wave height in as little as 3 h (Laing, 2001). Variability in coastline geomorphology, aspect, and bathymetry in this region interact with wind and swell, leading to energetic wave environments that vary greatly over a range of spatial (Jones et al., 2015) and temporal scales (Carter, 2008; Dunn, 2010). Nonetheless, empirical observations of this heterogeneity in nearshore environments is limited.

Hindcast WAM (WAve Models) models have estimated wave action with nearby wave rider buoys (Gorman et al., 2003), but these models are at a 1.125° × 1.125° latitude scale. Because coastal topography reduces the quality of model estimations at 'shallow' sites as deep as 30–40 m, the ability of this model to resolve wave dynamics applicable to the intertidal zone remains unclear. On the Wellington south coast, SWAN models (Simulating WAves Nearshore) have been used to estimate minimum, maximum, and mean orbital velocities (Jones et al., 2015), but to our knowledge there has not been a fine scale recorded time series of wave exposure data.

In this study, we estimate relative wave action on the Wellington south coast using HOBO acceleration loggers. Specifically, we aim to: (1) evaluate the sensitivity of *in situ* HOBO acceleration loggers to swell events recorded by a nearby wave rider buoy; (2) quantify fine-scale spatial variation in flow due to water depth; (3) determine the frequency of large wave events of the Wellington south coast over an extended (16 month) period of time; and (4) determine if an *a priori* categorization of sites as either wave 'sheltered' or 'exposed' (from direct observation of surface topography) is corroborated by acceleration data recorded *in situ*.

2. Materials and methods

2.1. Sites

We established six focal study sites that spanned putative gradients in wave exposure and hydrodynamic conditions. Site selections were informed by observations of shore aspect and topography during large swell events on the south coast. Three sites were selected to represent presumed 'sheltered' sites; these were located at the north side of Taputeranga Island (TI; 41°20′50.1″S, 174°46′23.4″E), the Island Bay inlet (IB; 41°20′54.4″S 174°46′05.7″E), and Moa Point (MP; 41°20′35.8″S 174°48′39.4″E; see open circles in Fig. 1). The remaining three sites were chosen to represent more 'exposed' locations; these were Yung Pen (YP; 41°20′58.8″S 174°45′15.3″E), Sirens Reef (SR; 41°20′58.3″S 174°45′51.4″E) and Princess Bay (PB; 41°20′42.2″S 174°47′12.4″E) (see filled circles in Fig. 1).

Substrate types across all sites included bedrock (continuous rock), boulders (>256 mm), cobbles (64–256 mm), rock (16–64 mm), gravel (4–16 mm), and sand (<4 mm; Connor et al., 2004; Laferriere, 2016). All sheltered sites contain an above-water rock buffer from waves, although the size and location of the buffer relative to shore differs at each site. Moa Point is sheltered by a small peninsula that curves in front of a small rocky beach. Deeper depths behind the peninsula are predominantly rock and shallow depths are predominantly sand. Taputeranga Island sits in front of the Island Bay Beach and provides shelter from southerly swells. The dominant substrate type at shallow depths is rock and at deeper depths is sand. Island Bay is a shallow channel buffered by an alongshore rocky reef. Deeper depths are predominantly gravel and shallow depths are predominantly rock. All of the 'exposed' sites are comprised of rocky reefs oriented perpendicular to shore. Yung Pen and Sirens Reef are mostly rock and cobble substrate. At deeper depths, Princess Bay is largely composed of sand and shallow depths are predominantly rock.

2.2. Recording water movement

HOBO acceleration loggers record acceleration in three axes (x-axis = vertical plane, y-axis = horizontal plane, z-axis = lateral plane). Acceleration magnitude for each axis is recorded with a positive or negative sign to distinguish the direction of movement. We chose the shortest possible sampling interval (5 min) to record frequent acceleration measurements while maintaining sufficient memory for longer deployments (up to 75 days). Loggers recorded acceleration in all three axes at a single point in time, and were recovered, downloaded and redeployed every 30–60 days for up to 16 months to facilitate a continuous time series of data.

Following the general methods detailed in Figurski et al. (2011), deployed loggers were positioned within a cylindrical waterproof housing (height: 22.5 cm x diameter: 6.5 cm) and attached to a short

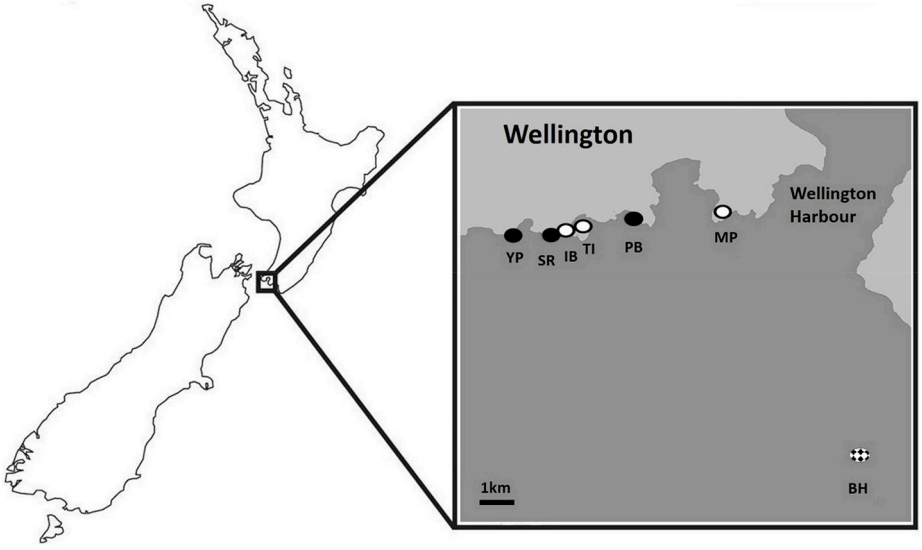

Fig. 1. Map of the focal study region along the south coast of Wellington, New Zealand. Filled circles mark areas hypothesised *a priori* to be 'exposed' sites (YP, SR, and PB); open circles mark areas hypothesised *a priori* to be 'sheltered' sites (IB, TI, and MP). NIWA's Baring Head buoy is marked with the patterned circle. At low tide, 'deep' moorings were 3.4–7.4 m deep. All 'shallow' moorings were 1–1.5 m deep at low tide.

mooring line (<50 cm length) affixed firmly to the substrate. Buoyancy was provided with a cylindrical foam insert (height: 10 cm x diameter: 6.5 cm, V: 355 mL, buoyancy (N): 3.586). Within each site, we deployed a single logger to each of two separate depths to evaluate hydrodynamic conditions in the subtidal zone (depth: 3.4–7.4 m) and a nearby intertidal zone (depth: 1–1.5 m). 'Deep' loggers were deployed in February 2016, and these recorded data continuously through July 2017 (516 days). 'Shallow' loggers were deployed in May 2016, and recorded data continuously through August 2017 (455 days), except for TI Shallow, which was deployed from April 2016 to July 2017 (470 days).

2.3. Data processing

We calculated a relative estimate of orbital velocity (*after* Figurski et al., 2011) for each day as the standard deviation of the magnitude of the accelerations, as:

$$\sigma\left(\sqrt{x^2+y^2+z^2}\right)$$

where σ denotes the standard deviation of a set of measurements from a given day (i.e., sampling at 5 min intervals yields n = 288 observations per 24 h period), and x, y, and z represent the accelerations in each axis recorded by the loggers in each interval. This calculation yields a robust summary of variable acceleration over time without requiring correction factors; this metric has also been shown to be unaffected by tilt errors (Figurski et al., 2011). Some loggers were deployed in areas frequented by beach-goers, and obvious outliers (e.g., consistent with someone handling the logger) were smoothed in the time series. We identified outliers of x, y, or z as values that exceeded twice the median of adjacent measurements; we replaced these values with an average of the three previous recordings (*after* Barbee and Swearer, 2007). This resulted in replacement of 33 data points (0.002%) of all data collected being replaced with the smoothed value.

2.4. Relationship between HOBO loggers and wave height

We compared the HOBO logger data with data obtained from a wave rider buoy (managed by the National Institute of Water and Atmospheric Research [NIWA]) deployed near the entrance of Wellington Harbour (41 24.6S, 174 50.9E) at Baring Head (BH; Fig. 1), 5 km from our sites. Records of Maximum Wave Height (m) and Significant Wave Height (m) were obtained for 66 random days (recorded at 30 min intervals; 3180 data points) from May 2016 to July 2017. Maximum wave height (H_{max}) is the maximum wave height recorded over time, and significant wave height is the average height of the highest one third of the waves over time. We correlated H_{max} and H_s from BH with half hour HOBO logger standard deviations of acceleration for each location using generalised least squares (GLS) models (24 models total: 12 locations compared with H_{max} and H_s). We included a spatial power correlation structure in the model to account for temporal autocorrelation in data with irregular time intervals between measurements (Wolfinger, 1993).

2.5. Comparison between sites and depths

We evaluated spatial variation in water acceleration among sites, depths, and their interaction using a GLS model. We included an autoregressive correlation structure in the model to account for temporal autocorrelation in the data (Agresti, 2007). We used Tukey tests to determine pairwise differences between sites and depths.

2.6. Characterising south coast temporal wave exposure trends

At all 12 locations, the frequency of large wave events for each season was calculated using the mean, across all locations, of the 95th percentile of daily standard deviations as the threshold. We identify days with large wave events as days when the standard deviation of water acceleration exceeded this threshold.

2.7. Evaluating proxies of wave exposure

We used *in situ* estimates of water acceleration to evaluate the efficacy of *a priori* classifications of wave exposure (i.e., sites were classified as either 'exposed' or 'sheltered' based upon coastal features observed from shore). Using only days when all loggers from all 12 locations were recording simultaneously (442), we undertook a hierarchical clustering analysis to group the 12 locations into wave exposure clusters. We first standardised the data (mean = 0, SD = 1), and then used the average linkage distance approach in our cluster analysis, as it is insensitive to outliers. We used the statistical software JMP (version 13.0.0) for this analysis.

Unless otherwise stated, analyses were performed using R 3.4.4 (R Core Team, 2017). We used the 'gls' function of the 'nlme' package for GLS models (Pinheiro et al., 2017) and the 'emmeans' and 'multcompView' packages for post hoc tests (Graves et al., 2015; Lenth, 2016). For all GLS models, models with and without a correlation structure were compared with maximum likelihood tests to confirm retaining the correlation structure in the model (Appendix A; Pekár and Brabec, 2016).

3. Results

3.1. Relationship between HOBO loggers and wave height

At all sites, H_{max} (maximum wave height; in metres) and H_s (significant wave height) were significantly associated with logger standard deviation (an index of wave action; Table 1), indicating a larger standard deviation of acceleration was associated with bigger swell.

3.2. Comparison between sites and depths

Standard deviation of acceleration varied among sites ($F_{(5,5829)} = 84.8837$, $p < 0.0001$; Fig. 2), but not consistently with water depth ($F_{(1,5829)} = 1.804$, $p = 0.1793$). The interaction between site and depth was significant ($F_{(5,5829)} = 73.919$, $p < 0.0001$), indicating that fine-scale variation in water acceleration (i.e., the pattern of variation across sites was dependent upon the placement of data recorders (shallow or deep) within a site; Fig. 3).

At IB, SR, and YP, deeper depths had significantly higher acceleration (Fig. 3). In contrast, at PB and TI, water acceleration was significantly greater at shallower depths. There was no significant difference between depths at MP. Deep sites significantly differed from one another among sites, apart from SR versus PB, TI versus IB, and YP versus PB and SR. At shallow depths, acceleration varied significantly between all sites.

3.3. Characterising south coast temporal wave exposure trends

Monthly distributions of large wave events (days above mean 95th percentile) varied dramatically at each location (Fig. 4). IB deep, IB shallow, SR shallow, TI deep and YP shallow experienced less than 1 large wave event per month and a maximum of 1 or 2 large wave events per month. All other locations experienced an average of 1.6–7 large wave events per month with a maximum of 5–13 large wave events per month. Eight of the twelve locations (IB shallow, MP shallow, PB shallow, SR deep, SR shallow, TI deep, TI shallow, and YP shallow) experienced the most large wave events in the winter months (June–August). The remaining four sites experienced the most large wave events in autumn (March–May) or spring (September–November).

3.4. Evaluating proxies of wave exposure

Formal clustering analysis of standard deviations calculated from logger data suggested two clusters of sites: 'exposed' and 'sheltered.' Fifty-eight percent of sites classified based on *a priori* observations were

Table 1
Results from GLS models comparing HOBO logger half-hour standard deviations of acceleration from each site with half hour measurements of significant (H_s) and maximum (H_{max}) wave height from BH (wave rider buoy at Baring Head). R^2 values were calculated from model fitted versus observed values.

H_s					H_{max}				
Site	Depth	χ^2	p-value	R^2	Site	Depth	χ^2	p-value	R^2
IB	Deep	30.3577	<0.0001	0.2812	IB	Deep	35.0545	<0.0001	0.2736
	Shallow	43.2696	<0.0001	0.1793		Shallow	28.61889	<0.0001	0.1697
MP	Deep	41.00733	<0.0001	0.2266	MP	Deep	44.75579	<0.0001	0.2139
	Shallow	90.6951	<0.0001	0.2097		Shallow	121.1449	<0.0001	0.213
PB	Deep	80.84211	<0.0001	0.2946	PB	Deep	134.7537	<0.0001	0.3022
	Shallow	109.3735	<0.0001	0.2756		Shallow	37.40308	<0.0001	0.2568
SR	Deep	23.98721	<0.0001	0.2076	SR	Deep	17.66905	<0.0001	0.2018
	Shallow	38.34964	<0.0001	0.0924		Shallow	26.49542	<0.0001	0.09133
TI	Deep	37.18578	<0.0001	0.19	TI	Deep	20.31437	<0.0001	0.179
	Shallow	27.17613	<0.0001	0.1509		Shallow	28.15067	<0.0001	0.147
YP	Deep	56.53051	<0.0001	0.338	YP	Deep	38.79341	<0.0001	0.3309
	Shallow	12.56862	0.0004	0.1367		Shallow	15.62946	0.0001	0.1388

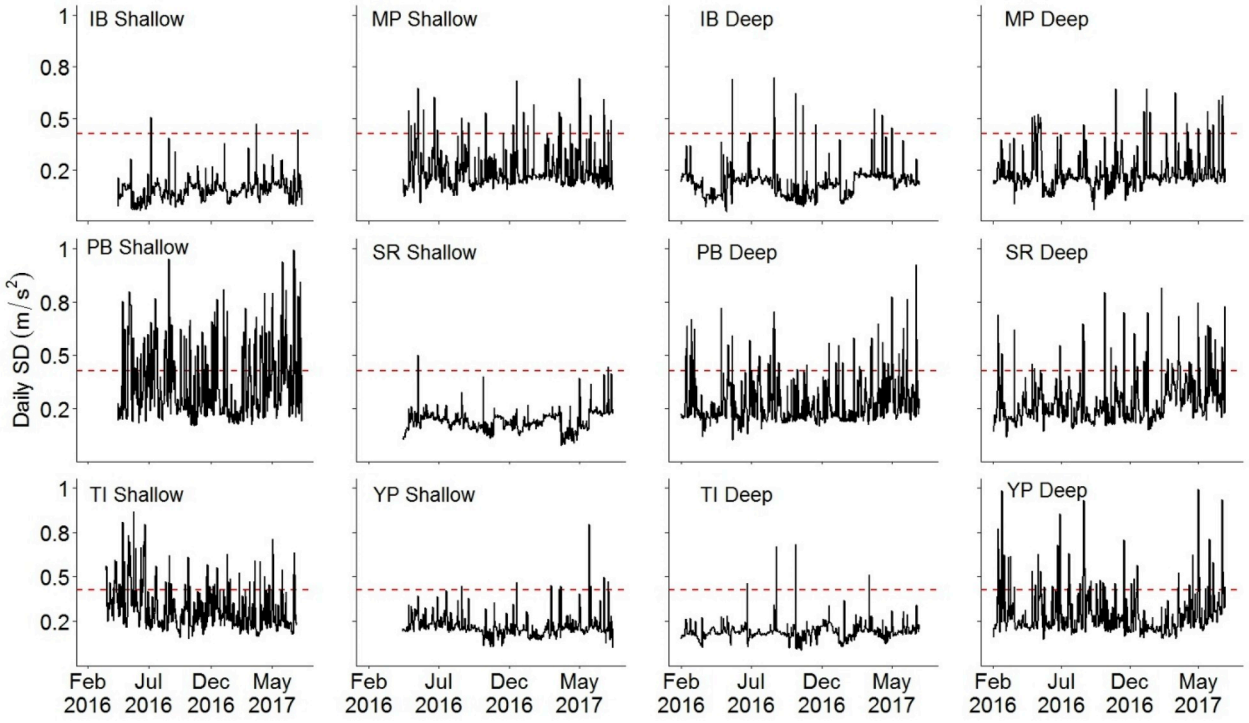

Fig. 2. Daily standard deviations of acceleration from each site (Princess Bay (PB), Moa Point (MP), Sirens Reef (SR), Taputeranga Island (TI), Yung Pen (YP), and Island Bay (IB)) and depth over 516 days. The dashed line represents the 95th percentile averaged across all twelve locations.

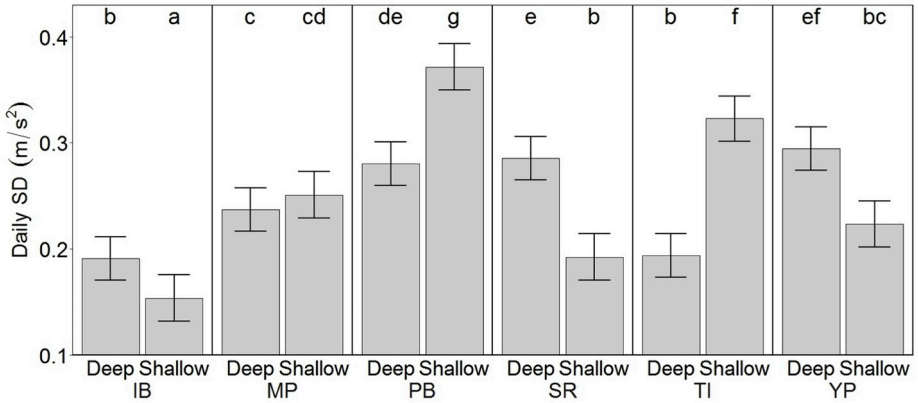

Fig. 3. Mean (±95%CI) standard deviation of acceleration for each site, estimated from the GLS model for the entire sampling period. Letters represent post-hoc Tukey test results. Sites with the same letters are not significantly different from one another.

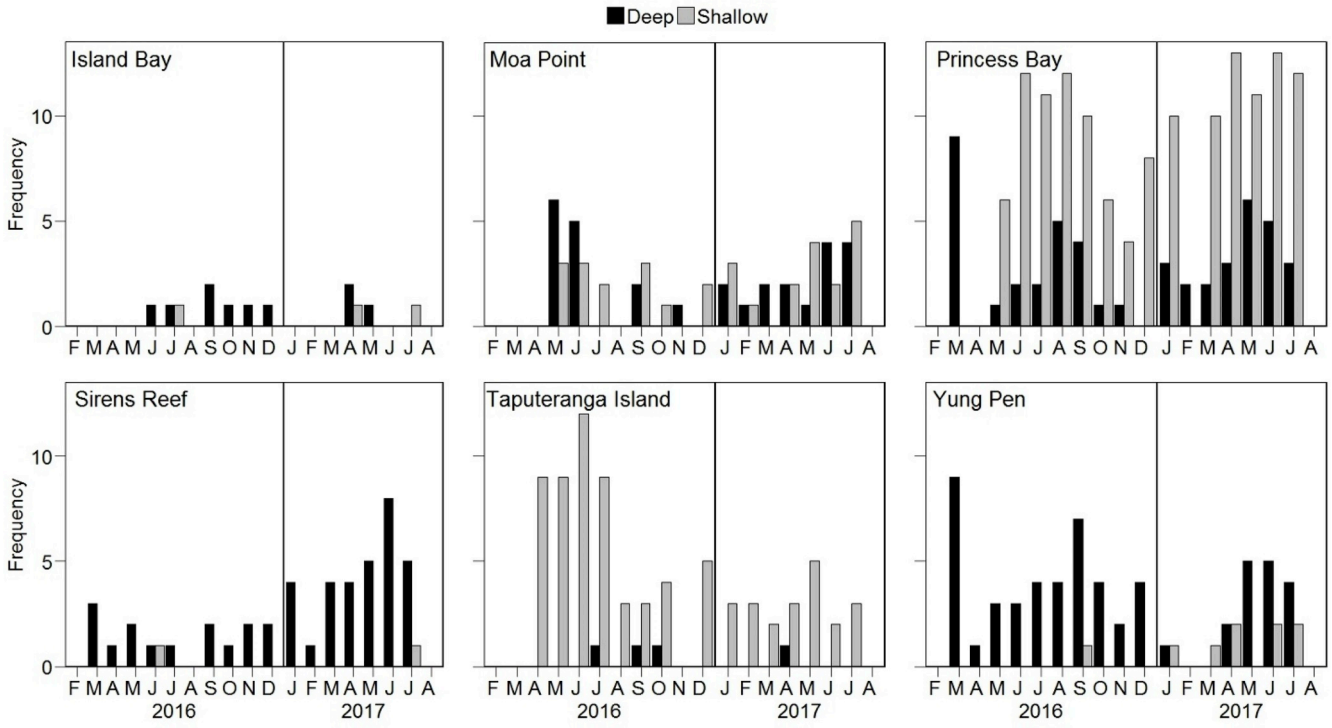

Fig. 4. Monthly frequency distributions of large wave events (days with standard deviation over the mean 95th percentile) across all 12 locations. Black bars denote deep locations and grey bars denote shallow locations.

similar to classifications based on clustering analysis (Table 2). Three sites initially categorised as sheltered were clustered into the exposed group (TI Shallow, MP Shallow and MP Deep); two sites initially categorised as exposed were clustered into the sheltered group (YP Shallow and SR Shallow). The analysis revealed that observed wave exposure was not strongly associated with depth. Over the entire time series, sheltered and exposed locations recorded similar minimum daily standard deviations (0.05 m/s^2 versus 0.06 m/s^2) with different maximum (0.79 m/s^2 versus 0.99 m/s^2) and mean (0.19 m/s^2 versus 0.29 m/s^2) standard deviations.

Table 2
Summary information for each location including (i) *A priori* exposure (*a priori* categorisations of wave exposed versus sheltered), (ii) observed exposure (cluster analysis categorisations of wave exposed versus sheltered determined from *in situ* acceleration) (iii) minimum daily standard deviation of acceleration recorded, (iv) calculated mean daily standard deviation of acceleration, and (v) maximum daily standard deviation of acceleration recorded. Bold text indicates sites where observed wave exposure was the same as *a priori* wave exposure.

Location (Site/ Depth)	*A priori* exposure	Observed exposure	Minimum (m/s^2)	Mean (m/s^2)	Maximum (m/s^2)
PB Shallow	**Exposed**	**Exposed**	0.17	0.37	0.99
TI Shallow	Sheltered	Exposed	0.16	0.32	0.86
YP Deep	**Exposed**	**Exposed**	0.15	0.29	0.99
SR Deep	**Exposed**	**Exposed**	0.12	0.29	0.81
PB Deep	**Exposed**	**Exposed**	0.10	0.28	0.92
MP Shallow	Sheltered	Exposed	0.09	0.25	0.69
MP Deep	Sheltered	Exposed	0.06	0.24	0.64
YP Shallow	Exposed	Sheltered	0.10	0.22	0.79
TI Deep	**Sheltered**	**Sheltered**	0.09	0.19	0.68
IB Deep	**Sheltered**	**Sheltered**	0.05	0.19	0.70
SR Shallow	Exposed	Sheltered	0.08	0.19	0.50
IB Shallow	**Sheltered**	**Sheltered**	0.05	0.15	0.51

4. Discussion

These results emphasise the spatial and temporal heterogeneity of flow experienced along the Wellington south coast. Five of the six sites recorded significant differences in daily mean water acceleration between depths. Water acceleration varied greatly among depths, as exemplified by significant differences among shallow (all 15) and deep locations (11 of 15) in pairwise comparisons. Locations were clustered into wave exposed or sheltered with no consistent relationship between site and depth. Frequency of large wave events dramatically differed across exposed and sheltered locations during the study period.

Variation in acceleration at each site may be explained by differences in local topography. Higher acceleration was recorded at IB, SR and YP at deeper depths (Fig. 3). Waves break at 0.78–1.4 times their height (Utter and Denny, 1996). Submerged reefs then dissipate wave friction and decrease wave energy from deep to shallow depths (Padilla-Hernández and Monbaliu, 2001), as evidenced by a 2.5 factor decrease in wave amplitude from deep to shallow wave gauges (Stevens et al., 2008). Conversely, at MP, PB, and TI, higher acceleration was recorded at shallow depths (Fig. 3), and likely driven by local conditions. For example, TI shallow was placed just north of Taputeranga Island, which presumably would provide shelter from southerly swells. However, there is a surge channel through the western side of the island that may have altered flow. Moreover, the influence of bedform drag on flow could explain differences between shallow sites (Stevens et al., 2008). Even though sites had similar substrate, subtleties in topography would alter friction and drag. To adequately record small-scale flow differences (e.g., over centimetres), loggers would need to be deployed within centimetres of one another (O'Donnell and Denny, 2008), which was not possible given our mooring construction.

Cluster analysis revealed that wave exposure was not limited to specific depths or sites. *A priori* exposure categorisations were based on wave observations considering rocks visible from the surface. Assessing wave exposure from visual estimation of emergent substrate does not take benthic topography or other processes of waves breaking

(refraction, diffraction, etc.) into consideration (Denny et al., 2003; O'Donnell and Denny, 2008; Jones, 2014). Tidal height also influences wave action. Emerging rocks attenuate the incoming waves at low tide at certain locations (e.g., SR shallow, R. Focht – unpublished data). Therefore, categorising exposure with visual estimation at different tidal heights may yield different results.

Acceleration data measured *in situ* (at a scale that is perhaps more relevant to organisms located in the sampled areas) was significantly correlated with the NIWA wave rider buoy data (i.e., bigger swell denotes a bigger standard deviation; Table 1) at all sites. In this study, moorings were 5 km away from the wave rider buoy supporting the assertion that these loggers are a cost-effective alternative to record accurate and precise wave exposure data (Figurski et al., 2011). Vortex shedding behind these instruments could have led to an overestimation of wave exposure; moorings were pulled towards the low pressure of water flowing around and behind them. However, acceleration data still significantly correlated with the wave rider buoy suggesting the potential influence of vortex shedding doesn't impede the ability of these loggers to provide a biologically meaningful measure of relative wave exposure. HOBO acceleration logger use *in situ* does have constraints. To record detailed metrics about waves, or to capture the entire wave cycle, measurements need to be recorded at high frequencies which requires large memory capacity and frequent servicing (Figurski et al., 2011). Consequently, when using these loggers, detailed wave measurements are sacrificed for longer deployments. Additionally, HOBO acceleration loggers only record movement when suspended in the water column. Since benthic organisms experience flow along the substrate, which is heavily influenced by friction and drag (Stevens et al., 2008), these loggers are limited in their ability to obtain detailed acceleration information on the substrate.

Despite the dramatic differences in large wave event frequency across sites, 11 of the 12 loggers recorded the most large wave events in autumn/winter, consistent with other studies in New Zealand (Dunn, 2010; Schiel et al., 2016). However, ten of the twelve loggers recorded large wave events in each of the seasons. For animals with a small home range, the difference in frequency of large wave events between exposed and sheltered sites (e.g., 1 per month versus 7 per month) has large implications for their life history. Timing and frequency of large wave events influences species distributions through displacement of individuals, as well as altering successional trajectories (Sousa, 1979). If large wave events occur in all seasons, organisms are likely to be influenced across multiple stages of their life history (Helmuth et al., 2006), which can lead to differences in morphology (Trussell, 2002), growth (McQuaid et al., 2000), and behaviour (Clarke et al., 2005).

For ecologists to understand how species cope with environmental fluctuations, it is necessary to understand the dynamic nature of the environment they inhabit. This is especially relevant with regards to potential climate change-mediated habitat perturbations. In the marine environment, annual increases in extreme wave heights (Young et al., 2011) and forecasted increases in storm intensity (Knutson et al., 2010) have the capacity to influence coastal ecosystems (Byrnes et al., 2011). Though models are improving in their capacity to estimate wave energy, there is limited nearshore data with which to compare their predictions (Dietrich et al., 2011; Jones, 2014). This study provides water acceleration measurements to elucidate temporal trends in wave exposure along the Wellington south coast at a scale relevant to intertidal/shallow subtidal organisms' home ranges.

Acknowledgements

P. Caie, D. Crossett, D. McNaughtan, C. Meyer, and M. Shaffer assisted with this research. The Greater Wellington Regional Council – Harbours Department gave permission to access the Wellington Harbour wave rider buoy data. L. Woods provided invaluable statistics guidance. The Victoria University Coastal Ecology Laboratory (VUCEL) provided logistical support. Funding was provided by a Marsden grant to J. Shima.

Appendix A

Table A.1.1
Likelihood ratio test results between generalised least squares (GLS) models. Each site/depth was correlated with wave rider buoy data from Baring Head with two models, one with a correlation structure and one without. Significant p values confirm the retaining a correlation structure in the model (n = 3180).

H_s					H_{max}				
Site	Depth	χ^2	df	p-value	Site	Depth	χ^2	df	p-value
IB	Deep	5718.672	1	<0.0001	IB	Deep	4646.812	1	<0.0001
	Shallow	6152.866	1	<0.0001		Shallow	5064.79	1	<0.0001
MP	Deep	5959.955	1	<0.0001	MP	Deep	4905.597	1	<0.0001
	Shallow	6074.427	1	<0.0001		Shallow	4982.389	1	<0.0001
PB	Deep	5709.28	1	<0.0001	PB	Deep	4617.634	1	<0.0001
	Shallow	5822.509	1	<0.0001		Shallow	4721.487	1	<0.0001
SR	Deep	6021.899	1	<0.0001	SR	Deep	4928.519	1	<0.0001
	Shallow	6467.59	1	<0.0001		Shallow	5349.253	1	<0.0001
TI	Deep	6105.04	1	<0.0001	TI	Deep	5020.592	1	<0.0001
	Shallow	6244.833	1	<0.0001		Shallow	5150.217	1	<0.0001
YP	Deep	5481.562	1	<0.0001	YP	Deep	4387.793	1	<0.0001
	Shallow	6282.708	1	<0.0001		Shallow	5167.853	1	<0.0001

Table A.1.2
Likelihood ratio test results comparing GLS models with and without a correlation structure. Model 1 tested for differences in daily standard deviation between locations and depths. Significant p values confirm retaining correlation structure in the overall model.

Model	n	χ^2	df	p-value
1	5842	311.5048	1	<0.0001

References

Agresti, A., 2007. Introduction to Categorical Data Analysis. Wiley, Hoboken, USA.

Barbee, N.C., Swearer, S.E., 2007. Characterizing natal source population signatures in the diadromous fish Galaxias maculatus, using embryonic otolith chemistry. Mar. Ecol. Prog. Ser. 343, 273–282.

Bell, E.C., Denny, M.W., 1994. Quantifying "wave exposure": a simple device for recording maximum velocity and results of its use at several field sites. J. Exp. Mar. Biol. Ecol. 181 (1), 9–29.

Bowman, M., Kibblewhite, A., Murtagh, R., Chiswell, S., Sanderson, B., 1983. Circulation and mixing in greater Cook Strait, New-Zealand. Oceanol. Acta 6 (4), 383–391.

Burrows, M.T., 2012. Influences of wave fetch, tidal flow and ocean colour on subtidal rocky communities. Mar. Ecol. Prog. Ser. 445, 193–207.

Byrnes, J.E., Reed, D.C., Cardinale, B.J., Cavanaugh, K.C., Holbrook, S.J., Schmitt, R.J., 2011. Climate-driven increases in storm frequency simplify kelp forest food webs. Glob. Chang. Biol. 17 (8), 2513–2524.

Caiger, P.E., 2017. The Effects of Habitat on Phenotype, Growth and Fitness in New Zealand Triplefin Fishes (Family: Tripterygiidae). Ph.D. Dissertation. University of Auckland.

Carter, L., 2008. Below low tide - a seabed in motion. In: Gardner, J., Bell, J. (Eds.), The Taputeranga Marine Reserve. First Edition Publishers Ltd, Wellington, New Zealand, pp. 130–144.

Chang, M.-H., Lien, R.-C., Yang, Y.J., Tang, T.Y., 2011. Nonlinear internal wave properties estimated with moored ADCP measurements. J. Atmos. Ocean. Technol. 28 (6), 802–815.

Clarke, R.D., Buskey, E.J., Marsden, K.C., 2005. Effects of water motion and prey behavior on zooplankton capture by two coral reef fishes. Mar. Biol. 146 (6), 1145–1155.

Connell, J.H., 1978. Diversity in tropical rain forests and coral reefs - high diversity of trees and corals is maintained only in a non-equilibrium state. Science 199 (4335), 1302–1310.

Connor, D.W., Allen, J.H., Golding, N., Howell, K.L., Lieberknecht, L.M., Northen, K.O., Reker, J.B., 2004. The marine habitat classification for britain and Ireland version 04.05. In: JNCC (2015) the Marine Habitat Classification for Britain and Ireland Version 15.03 [Online]. 1 April 2019. Available from: jncc.defra.gov.uk/MarineHabitatClassification.

Crimaldi, J.P., Thompson, J.K., Rosman, J.H., Lowe, R.J., Koseff, J.R., 2002. Hydrodynamics of larval settlement: the influence of turbulent stress events at potential recruitment sites. Limnol. Oceanogr. 47 (4), 1137–1151.

de Bettignies, T., Wernberg, T., Lavery, P.S., Vanderklift, M.A., Gunson, J.R., Symonds, G., Collier, N., 2015. Phenological decoupling of mortality from wave forcing in kelp beds. Ecology 96 (3), 850–861.

Denny, M.W., 2006. Ocean waves, nearshore ecology, and natural selection. Aquat. Ecol. 40 (4), 439–461.

Denny, M.W., Miller, L.P., Stokes, M., Hunt, L., Helmuth, B., 2003. Extreme water velocities: topographical amplification of wave-induced flow in the surf zone of rocky shores. Limnol. Oceanogr. 48 (1), 1–8.

Dietrich, J.C., Zijlema, M., Westerink, J.J., Holthuijsen, L.H., Dawson, C., Luettich, R.A., Jensen, R.E., Smith, J.M., Stelling, G.S., Stone, G.W., 2011. Modeling hurricane waves and storm surge using integrally-coupled, scalable computations. Coast Eng. 58 (1), 45–65.

Doty, M.S., 1971. Measurement of water movement in reference to benthic algal growth. Bot. Mar. 14 (1), 32–35.

Dunn, A.S., 2010. Coastal Storm Activity along the Eastern North Island of New Zealand - East Cape to Wellington. Ph.D. Dissertation. University of Waikato.

Evans, S.N., Abdo, D.A., 2010. A cost-effective technique for measuring relative water movement for studies of benthic organisms. Mar. Freshw. Res. 61 (11), 1327–1335.

Figurski, J.D., Malone, D., Lacy, J.R., Denny, M., 2011. An inexpensive instrument for measuring wave exposure and water velocity. Limnol Oceanogr. Methods 9 (5), 204–214.

Gaylord, B., 2000. Biological implications of surf-zone flow complexity. Limnol. Oceanogr. 45 (1), 174–188.

Gorman, R.M., Bryan, K.R., Laing, A.K., 2003. Wave hindcast for the New Zealand region: nearshore validation and coastal wave climate. N. Z. J. Mar. Freshw. Res. 37 (3), 567–588.

Graves, S., Piepho, H.-P., Selzer, L., Dorai-Raj, S., 2015. multcompView: Visualizations of Paired Comparisons. R package version 01-7.

Greene, C., Hall, J., Beamer, E., Henderson, R., Brown, B., 2012. Biological and Physical Effects of "Fish-friendly" Tide gates." National Oceanic and Admospheric Administation, National Marine Fisheries Service, Watersheds Program,. Northwest Fisheries Science Center, and Skagit River System Cooperative.

Harley, C.D., Helmuth, B.S., 2003. Local-and regional-scale effects of wave exposure, thermal stress, and absolute versus effective shore level on patterns of intertidal zonation. Limnol. Oceanogr. 48 (4), 1498–1508.

Harris, T.F.W., 1990. Greater Cook Strait: Form and Flow. DSIR Marine and Freshwater.

Helmuth, B., Broitman, B.R., Yamane, L., Gilman, S.E., Mach, K., Mislan, K., Denny, M. W., 2010. Organismal climatology: analyzing environmental variability at scales relevant to physiological stress. J. Exp. Biol. 213 (6), 995–1003.

Helmuth, B., Mieszkowska, N., Moore, P., Hawkins, S.J., 2006. Living on the edge of two changing worlds: forecasting the responses of rocky intertidal ecosystems to climate change. Annu. Rev. Ecol. Evol. Syst. 37 (1), 373–404.

Holthuijsen, L.H., Herbers, T.H.C., 1986. Statistics of breaking waves observed as whitecaps in the open sea. J. Phys. Oceanogr. 16 (2), 290–297.

Jokiel, P.L., Morrissey, J.I., 1993. Water motion on coral reefs: evaluation of the 'clod card' technique. Mar. Ecol. Prog. Ser. 93, 175–181.

Jones, T., 2014. Designing Accurate and Effective Means for Marine Ecosystem Monitoring Incorporating Species Distribution Assessments. Ph.D. thesis. Victoria University of Wellington.

Jones, T., Gardner, J.P.A., Bell, J.J., 2015. Modelling the effect of wave forces on subtidal macroalgae: a spatial evaluation of predicted disturbance for two habitat-forming species. Ecol. Model. 313, 149–161.

Knutson, T.R., McBride, J.L., Chan, J., Emanuel, K., Holland, G., Landsea, C., Held, I., Kossin, J.P., Srivastava, A.K., Sugi, M., 2010. Tropical cyclones and climate change. Nat. Geosci. 3 (3), 157–163.

Laferriere, A.A.M., 2016. Examining the Ecological Complexities of Blackfoot Paua Demography and Habitat Requirements in the Scope of Marine Reserve Protection. Victoria University of Wellington, Dissertation.

Laing, A.K., 2001. Rapid growth of waves on the east coast of New Zealand. Journal of Coastal Research Special Issue 34, 38–44.

Lenth, R.V., 2016. Least-squares means: the R package lsmeans. J. Stat. Softw. 69, 1–33.

Lewis, K.B., Carter, L., Davey, F.J., 1994. The opening of Cook Strait - interglacial tidal scour and aligning basins at a subduction to transform plate edge. Mar. Geol. 116 (3–4), 293–312.

Marchant, R., Stevens, T., Choukroun, S., Coombes, G., Santarossa, M., Whinney, J., Ridd, P., 2014. A buoyant tethered sphere for marine current estimation. IEEE J. Ocean. Eng. 39 (1), 2–9.

McQuaid, C., Lindsay, J., Lindsay, T., 2000. Interactive effects of wave exposure and tidal height on population structure of the mussel *Perna perna*. Mar. Biol. 137 (5–6), 925–932.

Menge, B.A., Sutherland, J.P., 1987. Community regulation - variation in disturbance, competition, and predation in relation to environmental-stress and recruitment. Am. Nat. 130 (5), 730–757.

O'Donnell, M.J., Denny, M.W., 2008. Hydrodynamic forces and surface topography: centimeter-scale spatial variation in wave forces. Limnol. Oceanogr. 53 (2), 579–588.

Padilla-Hernández, R., Monbaliu, J., 2001. Energy balance of wind waves as a function of the bottom friction formulation. Coast Eng. 43 (2), 131–148.

Pekár, S., Brabec, M., 2016. Marginal models via gls: a convenient yet neglected tool for the analysis of correlated data in the behavioural sciences. Ethology 122 (8), 621–631.

Pinheiro, J., Bates, D., DebRoy, S., Sarkar, D., R Core Team, 2017. Nlme: Linear and Nonlinear Mixed Effects Models. R package version 31-131.

R Core Team, 2017. R: A language and environment for statistical computing. R Foundation for Statistical Computing, Vienna, Austria. https://www.R-project.org/.

Radermacher, M., Thackeray, Z., De Schipper, M., Gordon, L., Chrystal, C., Leuci, R., Reniers, A., 2015. Tilt Current Meter Array: Field Validation. IAHR.

Schiel, D.R., Lilley, S.A., South, P.M., Coggins, J.H., 2016. Decadal changes in sea surface temperature, wave forces and intertidal structure in New Zealand. Mar. Ecol. Prog. Ser. 548, 77–95.

Sousa, W.P., 1979. Disturbance in marine inter-tidal boulder fields - the non-equilibrium maintenance of species-diversity. Ecology 60 (6), 1225–1239.

Speransky, S.R., Brawley, S.H., Halteman, W.A., 2000. Gamete release is increased by calm conditions in the coenocytic green alga Bryopsis (Chlorophyta). J. Phycol. 36 (4), 730–739.

Stevens, C., Taylor, D., Delaux, S., Smith, M., Schiel, D., 2008. Characterisation of wave-influenced macroalgal propagule settlement. J. Mar. Syst. 74 (1–2), 96–107.

Tam, J.C., 2012. Intertidal Community Differences between the Cook Strait and Wellington Harbour. Ph.D. thesis. Victoria Univeristy of Wellington.

Taylor, D., Delaux, S., Stevens, C., Nokes, R., Schiel, D., 2010. Settlement rates of macroalgal algal propagules: cross-species comparisons in a turbulent environment. Limnol. Oceanogr. 55 (1), 66–76.

Trussell, G., 2002. Evidence of countergradient variation in the growth of an intertidal snail in response to water velocity. Mar. Ecol. Prog. Ser. 243, 123–131.

Utter, B., Denny, M., 1996. Wave-induced forces on the giant kelp *Macrocystis pyrifera* (Agardh): field test of a computational model. J. Exp. Biol. 199 (12), 2645–2654.

Wolfinger, R., 1993. Covariance structure selection in general mixed models. Commun. Stat. Simulat. Comput. 22 (4), 1079–1106.

Young, I., Zieger, S., Babanin, A.V., 2011. Global trends in wind speed and wave height. Science 332 (6028), 451–455.